Minimum leaf conductance during drought: unravelling its variability and impact on plant survival

Régis Burlett, Santiago Trueba, Xavier P. Bouteiller, Guillaume Forget, José M Torres-Ruiz, Nicolas Martin-StPaul, Camille Parise, Hervé Cochard, Sylvain Delzon

New Phytologist

Research

Minimum leaf conductance during drought: unravelling its variability and impact on plant survival

Régis Burlett[1]*, Santiago Trueba[1,2]*, Xavier Paul Bouteiller[1], Guillaume Forget[1], José M. Torres-Ruiz[3], Nicolas K. Martin-StPaul[4], Camille Parise[1], Hervé Cochard[5] and Sylvain Delzon[1]

[1]INRAE, UMR BIOGECO, Université de Bordeaux, Pessac, 33615, France; [2]AMAP, Université de Montpellier, CIRAD, CNRS, INRAE, IRD, Montpellier, 34398, France; [3]Instituto de Recursos Naturales y Agrobiología de Sevilla (IRNAS), Consejo Superior de Investigaciones Científicas (CSIC), Seville, 41012, Spain; [4]INRAE, UEFP, Avignon, 84914, France; [5]INRAE, PIAF, Université Clermont Auvergne, Clermont-Ferrand, 63000, France

Author for correspondence:
Régis Burlett
Email: regis.burlett@u-bordeaux.fr

Received: *7 October 2024*
Accepted: *15 February 2025*

New Phytologist (2025)
doi: 10.1111/nph.70052

Key words: cuticular conductance, drought stress, relative water content, stomatal closure, turgor loss point, water potential.

Summary

- Leaf water loss after stomatal closure is key to understanding the effects of prolonged drought on vegetation. It is therefore important to accurately quantify such water losses to improve physiology-based models of drought-induced plant mortality.
- We measured water loss of detached leaves continuously during dehydration in nine woody angiosperm species. We computed minimum leaf conductance (g_{min}) at different water potential thresholds along a sequence of physiological function losses, spanning from turgor loss point to hydraulic failure. A mechanistic model evaluated the impact of different g_{min} estimations on the time to hydraulic failure (THF).
- Residual conductance is not steady and decreases continuously at varying rates across species during the entire dehydration process, even after correcting for leaf shrinkage and vapor pressure deficit shifts. Different estimations of g_{min} had a significant impact on the THF predicted by the model, especially for drought-resistant species.
- We demonstrate that residual conductance is variable during dehydration, and thus, it is important to use physiological or water status boundaries for its estimation in order to determine distinct g_{min} values of water loss. We describe an accurate, repeatable and open-source methodology to estimate g_{min}. Such methodology could enhance models of plant mortality under drought.

Introduction

In the last few decades, a large number of studies have brought to light the particular threat of drought and increasing temperatures on plant survival (Allen & Breshears, 1998; Carnicer *et al.*, 2011; Brodribb *et al.*, 2019; Hammond *et al.*, 2022). One of the main consequences of increasing environmental drought stress is a negative impact on the hydraulic function of plants (Choat *et al.*, 2012; Arend *et al.*, 2021). Indeed, during prolonged drought, dehydration causes large water potential differences between soil and leaves, which can result in hydraulic dysfunction due to embolism formation in the xylem conduits. Such hydraulic failures, induced by sharp drops in water potential, can be avoided through stomatal closure (Creek *et al.*, 2020), which plays a major role in plant survival under drought (Martin-StPaul *et al.*, 2017). Despite stomatal closure being a key reaction to reduce significant plant water losses, water is still lost through imperfectly closed stomata and the leaf cuticle. This process can be quantified by the minimum leaf conductance (g_{min}) (Duursma *et al.*, 2018). Although the rates of whole-plant water conductance are greatly diminished, g_{min} can be sufficient to deplete the plant water reserves during stress. Therefore, under prolonged drought, continued water loss via g_{min} can lead to catastrophic hydraulic failure and substantial tissue dehydration that contribute to organ and plant death (Urli *et al.*, 2013; Mantova *et al.*, 2023; Petek-Petrik *et al.*, 2023). Consequently, g_{min} has been highlighted as an important trait in predicting whole-plant transpiration and water status under severe stress (Barnard & Bauerle, 2013; Kala *et al.*, 2016). More recently, g_{min} has been advanced as a key trait to predict the time taken by a plant to reach hydraulic failure (THF) and subsequent mortality during drought (Cochard *et al.*, 2021; Ruffault *et al.*, 2022a; Petek-Petrik *et al.*, 2023) and to predict other current hazards to vegetation such as wildfire incidence (Ruffault *et al.*, 2022b; Torres-Ruiz *et al.*, 2024).

Synthetic studies gathering g_{min} data showed that estimations of residual transpiration in the literature come from a wide

*These authors contributed equally to this work.

variety of experimental techniques (Kerstiens, 1996; Duursma *et al.*, 2018). While cuticular conductance on isolated cuticles has been measured since early studies (Stålfelt, 1956; Schönherr & Mérida, 1981; Pearcy *et al.*, 1989), only a few protocols to measure g_{min} on a full leaf have been tested. Generally, measurement protocols rely on evaluating water loss through balance-based mass estimations over time and selecting the slope of the relationship between mass and time after the point of stomatal closure, assuming that water losses through the cuticle are steady as the leaf dehydrates (Sack & Scoffoni, 2010) or through water vapor conductance measurements using custom gas exchange systems (Boyer *et al.*, 1997; Márquez *et al.*, 2022). Automated devices have recently been developed in order to provide continuous measurements of water loss during dehydration under constant environmental conditions (Billon *et al.*, 2020). Yet, to date, no study has estimated potential shifts in leaf water conductance during the entire desiccation process. Furthermore, intrinsic factors can provoke shifts in water conductance estimations. Among these factors, leaf shrinkage or leaf rolling during dehydration can significantly impact the estimation of leaf hydraulic traits (Scoffoni *et al.*, 2014); hence, variations in leaf area need to be considered in conductance calculations. Additionally, water potential decline during leaf dehydration can also slightly influence conductance rates by affecting the water vapor pressure (vapor pressure deficit, VPD) inside the leaf and therefore the driving force for transpiration between the leaf and the atmosphere (Nobel, 2009).

Using a dynamic approach to estimate residual water losses during the entire dehydration process, and including phenomena that are often neglected in leaf conductance estimations, such as leaf shrinkage and water potential-induced VPD changes, this study aimed to assess the dynamics of residual leaf water conductance during dehydration. By measuring its variability during dehydration, this work also aimed to strictly distinguish residual conductance (g_{res}) as a dynamic water loss during dehydration after stomatal closure, and g_{min} as conductance values bounded by physiology-informed boundaries. We therefore capture variable residual conductance by measuring g_{min} at specific thresholds. Because of the key role of g_{min} in the depletion of the last vital water reserves of the plant after stomatal closure, there is a need to use repeatable and reliable protocols for its estimation. Here, we describe a complete methodology to investigate g_{min} based on continuous measurements of relative water content (RWC) over time. Moreover, we use water status- and physiology-based thresholds to determine g_{min}. We provide detailed information on the device and open-source software used to analyze data. By applying this new technique to a selection of nine species with various phenologies, water use strategies, and resistances to drought, we will (i) test the hypothesis that residual conductance after stomatal closure varies along a gradient of declining water potential and RWC, (ii) assess how this variation affects the estimation of g_{min} at physiologically relevant thresholds distributed along a temporal sequence, and (iii) investigate how the range of g_{min} estimated along this drought physiological time sequence can influence model outcomes of plant survival under drought stress.

Materials and Methods

Plant material and species selection

We selected nine woody angiosperm species with different phenologies (five deciduous and four evergreen) and resistances to drought (Table 1). Six- to 7-yr-old saplings with heights of *c.* 2 m were obtained from local nurseries and planted in 30 l pots with a fertilized substrate. Plants were placed in a climate-controlled glasshouse in March 2019 (before leaf expansion) and kept irrigated to field capacity during the whole experiment. In September 2019, five sampling campaigns were performed on well-watered plants during the morning. Mature leaves, located at the top of the trees, were cut at the base of the petiole. This cut end was immediately placed in a water-filled reservoir, and the leaves were left to rehydrate for at least 8 h in the dark in a coolbox with vapor-saturated air using previously established rehydration protocols (Trueba *et al.*, 2019).

Measurements of water loss and relative water content

Water loss measurements of detached leaves were performed with a custom setup using similar data acquisition hardware to the *droughtbox* device (Billon *et al.*, 2020). Weight loss was monitored by continuous logging of micro-load cells using a Wheatstone bridge board (1046_OB; Phidgets Inc., Calgary, AB, Canada). Our setup consisted of 24 load cells, with a range of 0–100 g (3139_0; Phidgets Inc.) enclosed in a commercially available 1200 l growing chamber (Fitoclima 1200, Aralab, Portugal). Temperature and relative humidity (RH) in the chamber were set to 25°C and 60%, respectively, resulting in an air VPD of *c.* 1.26 kPa. During measurements, samples were illuminated from the top and the bottom with a photon flux density of 400 µmol m^{-2} s^{-1}. The base of the petiole was covered in paraffin wax before entering the chamber to prevent direct desiccation from the cut end. Samples were automatically weighed every 5 min. Custom software (Cuticular v1, University of Bordeaux) was developed to handle data acquisition, calibration, and metadata management. More details of the measurement system are available in Supporting Information Methods S1.

The measuring system designed in this study provided a resolution of the load cell acquisition system of 0.001 g with a typical instant standard deviation of 0.033 g (5 min average). The relatively big difference between resolution and standard deviation is mostly explained by the movement of the samples caused by the ventilation in the chamber. The measured signal-to-noise ratio is typically 77 at 2 g and 260 at 8 g. The long-term temperature drift remained below 0.03°C d^{-1}, and the long-term RH drift was below 0.08% d^{-1}. Further information on data acquisition and system performance is available in Methods S1.

Turgid weight (TW) and area (A_{leaf}) of each individual leaf were measured before the water loss measurements in the climatic chamber. Weight measurements were performed with a 4-digit balance (Pioneer, Ohaus, USA). Leaf area was obtained from images taken with a calibrated flatbed scanner (v850 pro; Epson,

Table 1 List of the nine species studied including physiological variables.

Species	Family	Phenology	Species code	π_0 (MPa)	ε MPa	RWC_TLP (%)	RWC_P_{12} (%)	RWC_P_{50} (%)	RWC_P_{88} (%)	Succulence (g m^{-2})	Symplast fraction (%)	Hydraulic safety margin (MPa)
Fraxinus excelsior L.	Oleaceae	Deciduous	FREX	−1.56	10.93	83.9	28.7	25.2	22.5	105.1 ± 2.1	76.6 ± 1.8	−5.47
Liriodendron tulipifera L.	Magnoliacea	Deciduous	LITU	−1.41	10.95	84.2	72.8	67.1	62.2	139.1 ± 4.3	61.4 ± 3.1	−0.85
Magnolia grandiflora L.	Magnoliacea	Evergreen	MAGR	−1.37	7.63	78.2	53.6	48.3	44	228.6 ± 1.4	75.8 ± 2.6	−1.75
Olea europaea L.	Oleaceae	Evergreen	OLEU	−2.11	12.65	83.4	38.7	36.8	35.1	238.0 ± 2.5	83.9 ± 4.3	−3.91
Prunus avium L.	Rosaceae	Deciduous	PRAV	−1.90	12.05	83.0	51.8	42.2	35.6	117.1 ± 0.8	65.5 ± 2.5	−3.43
Prunus laurocerasus L.	Rosaceae	Evergreen	PRLA	−1.65	14.02	87.0	40.0	33.1	28.2	231.1 ± 1.7	50.6 ± 3.2	−4.21
Quercus ilex L.	Fagaceae	Evergreen	QUIL	−1.93	8.16	73.4	37.7	27.1	21.2	198.6 ± 5.5	73.2 ± 1.4	−7.20
Quercus robur L.	Fagaceae	Deciduous	QURO	−1.72	11.27	81.6	43.0	36.2	31.3	124.1 ± 1.6	80.4 ± 2.9	−3.77
Vitis vinifera L.	Vitaceae	Deciduous	VIVI	−1.29	7.73	79.0	63.6	58.7	54.5	126.3 ± 3.8	74.4 ± 2.1	−1.08

π_0, osmotic potential at full turgor; ε, modulus of elasticity; RWC_TLP, relative water content at turgor loss point; RWC_P_{12}, relative water content at 12% loss of hydraulic conductivity; RWC_P_{50}, relative water content at 50% loss of hydraulic conductivity; RWC_P_{88}, relative water content at 88% loss of hydraulic conductivity. Physiological variables used as inputs for the SurEau model and units for each variable are included. Reported error values are SE.

Suwa, Japan) and analyzed with dedicated software (Winfolia, Regent Inst., Canada). At the end of the measurement, leaves were placed in an oven at 65°C for 72 h, and dry weight (DW) was measured. The RWC was then computed for each mass value (fresh mass; FW) during the dehydration process using Eqn 1:

$$\mathrm{RWC} = 100 \times \frac{\mathrm{FW}-\mathrm{DW}}{\mathrm{TW}-\mathrm{DW}} \qquad \text{Eqn 1}$$

Computation of minimum and residual leaf conductance

Minimum and residual conductance were computed for each leaf as the water evaporation rate divided by its driving force (VPD), using Eqn 2:

$$g_{\min} = \frac{\mathrm{d}w/\mathrm{d}t}{M_{H_2O} \times A_{\mathrm{leaf}}} \times \frac{P_{\mathrm{atm}}}{\mathrm{VPD}} \qquad \text{Eqn 2}$$

where $\mathrm{d}w/\mathrm{d}t$ is the first derivative of the curve of the hourly mean of weight (in g) as a function of time (in s), M_{H_2O} is the molecular weight of water (18.01 g mol^{-1}), A_{leaf} is the projected leaf area of the sample (in m^2), P_{atm} is the atmospheric pressure in the chamber (*c.* 101.9 kPa), and VPD is the vapor pressure deficit between the substomatal cavity and the air inside the chamber (in kPa). To compute minimum conductance in a reproducible and efficient manner, console-based software was developed in Python (*gminComputation*, University of Bordeaux) and also implemented as an R script (*g_Residual*, University of Bordeaux). Both software are available in the repository: https://gitub.u-bordeaux.fr/phenobois. The computation pipeline automatically performs a finite impulse response smoothing filter, using the Savitzky–Golay method. This method uses polynomial model fitting to determine the averaged mass and computes the derivative within a given time frame to estimate the conductance every hour or within a set of given ranges of RWC. For all the dehydration curves in this study, we applied a centered 120 min filter and used a third-order polynomial to fit each curve (Methods S1).

Measurements of hydraulic traits from pressure–volume curves

For each species, the water potentials of the leaves during the conductance measurements were estimated from the relationship between RWC and water potential obtained from pressure–volume (PV) curves (Tyree & Hammel, 1972). PV curves were performed on a set of 7–12 leaves collected in the evening on well-watered potted plants and left to rehydrate overnight in the dark. The next day, the leaves were weighed just before water potential was measured with a pressure chamber (Precis 2000, Gradignan, France). Samples were then left to dehydrate at room conditions, and the measurements were repeated 10–20 times until water potential dropped significantly below the turgor loss point (TLP). Elasticity modulus (ε) and osmotic potential at full turgor (π_0) were determined using a standard protocol (Sack *et al.*, 2010). Results of the parameters extracted from the PV curves for each species are available in Table 1. Additionally, the Hydraulic stomatal Safety Margin (HSM) for each species was computed, using the definition from Delzon & Cochard (2014), as the difference between the water potential inducing stomatal closure ($P_{\mathrm{close}} = P_{\mathrm{TLP}}$, defined as the value of water potential at TLP) and the water potential inducing a lethal level of embolism ($P_{\mathrm{lethal}} = P_{88}$, defined as the value inducing 88% of embolism in the stem). HSM values for each species are available in Table 1.

Leaf shrinkage measurements

For each species, seven leaves of different sizes were placed on a flatbed scanner (v850 pro, Epson, Japan), with the lid slightly ajar to allow for potential leaf rolling. A custom automation script (autoIT) was used to launch the image acquisition and record time-coded images every 15 min. Individual leaf areas were obtained for each image in the stack with the 'batch mode' of image analysis software (Winfolia, Regent Inst., Canada). For each leaf, the weight was measured regularly with a precision balance (Pioneer, Ohaus, USA) and RWC estimated following the previously described protocol (Eqn 1) until RWC reached 30%,

assuming that below this threshold leaves lose rehydration capacities and present irreversible damage to the photochemical apparatus (Trueba *et al.*, 2019). The percentage of shrinkage was determined for each species by fitting a 4-degree polynomial on the relation of the percentage of area loss as a function of RWC (Table S1). This polynomial has been used, for each RWC level, to sequentially correct the leaf area values used in the g_{min} computation.

Leaf to air vapor pressure deficit correction

As leaves dehydrate, the water potential decreases, which impacts the water vapor pressure (P_{wv}) in the substomatal cavities, thereby affecting the VPD between leaf and air ($VPD_{leaftoair}$). While negligible for hydrated leaves, this phenomenon needs to be taken into account for the computation of conductance during more intense dehydration. If we assume that the air in the intercellular air space of the mesophyll is in equilibrium with the liquid water at the surface of the mesophyll cells, we can determine the water potential of the water vapor in the gas phase (Ψwv) of the air in the substomatal cavities (Nobel, 2009; Vesala *et al.*, 2017) using Eqn 3:

$$\psi_{wv} = \frac{RT}{V_w} \log_e \frac{P_{wv_{inleaf}}}{P^*_{wv}} \quad \text{Eqn 3}$$

where ψ_{wv} is the water potential of the water vapor, V_w is the molar volume of water (18×10^{-6} m^3 mol^{-1}), R is the universal gas constant, T is the interfacial temperature (K), P_{wv} is the water vapor pressure, and P^*_{wv} is the water vapor pressure at saturation. In this study, the interfacial temperature is assumed to be in equilibrium with air temperature, as the cooling effect of transpiration is negligible (below 0.2°C) in the conditions of the measurement. From this equation, we can estimate $VPD_{leaf\text{-}to\text{-}air}$ using Eqn 4:

$$\begin{aligned} VPD_{leaftoair} &= P_{wv_{inleaf}} - P_{wv_{inair}} \\ &= \left(P^*_{wm} \times \exp\left(\frac{V_w}{RT} \psi_{wv} \right) \right) - P_{wv_{inair}} \end{aligned} \quad \text{Eqn 4}$$

For all conductance estimations in this study, this value of VPD corrected for water potential ($VPD_{leaftoair}$) was used instead of the air VPD as defined in Eqn 2, unless specified otherwise.

Different approaches to determine the range of g_{min} measurements

Under the assumption that residual conductance is variable, we need to consider which value has to be used for comparing species and how this variation can be taken into account in the parameterization of the models. For that, we assessed four different exploratory methods to determine g_{min}, extracting slope values at different ranges of the mass–RWC relation in the curves of dehydrating leaves: (1) A first physiology-based approach consisted of the calculation of g_{min} using the slope (dw/dt) at RWC_{TLP}, under the hypothesis that TLP is a close *proxy* of stomatal closure (Brodribb & Holbrook, 2003). (2) A second approach consisted in calculating g_{min} using the slope at the major points along stem vulnerability to embolism curves, previously established with the cavitron technique (Cochard, 2002; Burlett *et al.*, 2022). For all those points, we used stem vulnerability, rather than leaf, curves because they are more commonly available. The threshold values we used correspond to the water potentials inducing 12%, 50%, and 88% losses of conductance in the stem (respectively P_{12}, P_{50}, and P_{88}) under the rationale that hydraulic failure occurs around those water status levels (Sperry *et al.*, 1988), between P_{12} (beginning of embolism) and P_{88} (the threshold inducing mortality). Moreover, estimating g_{min} at different thresholds of hydraulic failure was also a way to control for the lack of stomatal activity, since it has been shown that stomatal closure occurs well before embolism initiation (Lamarque *et al.*, 2018; Creek *et al.*, 2020). In order to estimate the RWC corresponding to these points (respectively RWC_P_{12}, RWC_P_{50}, and RWC_P_{88}), we used the relationship between RWC and water potential obtained from the PV curves. (3) A third approach to estimate g_{min} was by extracting the slope between the thresholds of RWC inducing stomatal closure (*c.* 80%) and the loss of rehydration capacity (*c.* 50%) based on a previous study (Trueba *et al.*, 2019). Such boundaries were also established under the assumption that a water potential of −4 MPa represents a boundary of absolute stomatal closure (Martin-StPaul *et al.*, 2017), which is concomitant to *c.* 80% RWC according to PV curves performed in this study. This approach was implemented in order to use conservative boundaries that could be applied *a priori* across plant species without preexisting physiological assessments. The values of g_{min} obtained using the previously described methods were compared in order to assess their potential dissimilarities. (4) A fourth approach consisted in estimating g_{min} in 10% ranges from 100% to 0% RWC. These ranges were used to estimate conductance dynamically, including corrections for leaf shrinkage and leaf-to-air VPD. Such an approach allowed us to understand at which stages of dehydration shrinkage and VPD variation had a major impact on residual conductance.

Determination of time to hydraulic failure with various g_{min} values

Time to hydraulic failure (THF) is often defined as the time required by a plant to reach a RWC value corresponding to a loss of 88% of hydraulic conductance (RWC_{P88}). This level of water stress has been previously shown to correspond to a threshold inducing plant mortality in angiosperm species (Urli *et al.*, 2013; Li *et al.*, 2016). For each species, RWC_{P88} has been estimated using PV relationships and vulnerability curves. The time to reach this 88% threshold (THF_observed) was then directly measured for each individual detached leaf inside the *droughtbox*, during the dehydration experiment. This measurement was used as a reference.

Additionally, the model SurEau (Cochard *et al.*, 2021) has been used to estimate, at the leaf level, THF using different values of g_{min} computed with the different thresholds previously described. Namely: THF_TLP, THF_P_{12}, THF_P_{50}, THF_P_{88}, and

THF_RWC$_{80\text{-}50}$. An additional approach taking into account the continuous variability of g_{min} has also been implemented in the model (THF_variable). The dynamics of g_{min} was estimated using a segmented linear model in the equation $g_{min} = f(RWC)$. In short, the variation of g_{min} was assumed constant before stomatal closure (i.e. between RWC$_{100\%}$ and RWC_TLP) and decreased linearly after stomatal closure. In practice, the slope of the function between RWC_TLP and RWC$_{30\%}$ was used to estimate g_{min}. Coefficients of the linear fit for each species can be found in Table S1. In all simulations, model computation was performed with the following hypotheses: (1) leaves remain connected to the stem throughout the dry down, and (2) hydraulic vulnerability curves are similar for leaves and stems.

SurEau model parameterization

Simulations of THF were performed for each species using averaged values of each leaf-related trait. These values can be found in Tables 1 and S1. The degree of succulence was estimated by the ratio of fresh weight to leaf area (Delf, 1912) on a set of at least 10 hydrated leaves. The symplastic water fraction (SWF) was estimated from the PV curve (Koide *et al.*, 2000) with Eqn 5:

$$\frac{1}{\psi} = a * (100 - \mathrm{RWC}) + b \qquad \text{Eqn 5}$$

where ψ is the water potential (in MPa), RWC is the relative water content (in kg kg^{-1}), and a and b are the slope and intercept of the linear part of the PV curve (RWC < 80%), respectively. In short, we extrapolated the PV curve function to estimate the RWC deficit at a low water potential, which gives a direct estimation of the SWF. The apoplastic water fraction was defined as 100 − SWF.

Statistical analyses

Assumptions of residual homogeneity and normality were tested before analyses. Correlation analyses were used to assess relationships between PV curve parameters and g_{min} values estimated with different physiological thresholds. A model explaining the variance of percent leaf area, including the interaction RWC × species, was also performed to assess whether RWC had an effect on leaf shrinkage across all species. Bivariate linear regressions were used to estimate relationships between modelled and measured THF. Similarly, linear models were used to assess the prediction of safety margins from the THF. All analyses were considered significant at $\alpha = 0.05$. All statistical analyses, data treatment, and graphics were performed using R v.4.3.2 (R Core Team, 2022).

Results

Leaf mass decline and shrinkage during dehydration

Continuous measurements of mass loss using 5 min intervals provided extensive dehydration curves (Fig. S1). Most of the species showed exponential declines in RWC over time, starting with a steep decrease, followed by a gradual slope flattening (Fig. 1). Species showed overall declines in projected leaf area during dehydration (Fig. 2). Species varied significantly in their shrinkage under dehydration (one-way ANOVA; $P \leq 0.001$; Table S1). Although the onset of leaf shrinkage started early during dehydration in some species, more significant leaf area reductions were observed after RWC_TLP, the RWC at turgor loss (Fig. 2). Across species, *Magnolia grandiflora* had the least shrinkable leaves, decreasing only by 3% on average across the dehydration process, while *Olea europaea* showed the strongest decline in projected leaf area, with a 37% reduction across the entire RWC decline, mostly because of a strong curling occurring after 50% of RWC. A model explaining leaf shrinkage variance, including the RWC interval × species interaction, showed that species explained shrinkage variations better than RWC, when considered at similar RWC intervals (Table S2), implying that a larger fraction of the leaf shrinkage variation, at a given RWC, was explained by attributable differences in leaf structure across species.

Dynamics of residual conductance during leaf dehydration

Continuous measurements of leaf water conductance over declining RWC showed that residual conductance varied greatly during dehydration (Fig. 3). For every species, such conductance declines were mostly driven by a decline in dw/dt, and these declines persisted even after g_{min} values were corrected for leaf shrinkage and leaf-to-air VPD (Fig. 3). None of these corrections showed significant differences with raw g_{min} estimations ($P > 0.6$ for each pairwise comparison). Leaf water conductance variations persisted after the TLP, which was assumed here to correspond to the point of stomatal closure. Between the point of stomatal closure (RWC_TLP) and the point of desiccation (defined previously as the point at which RWC reaches 30%), we observed a linear decrease of g_{min} as RWC decreased (Fig. 3). The slope of this decline in g_{min} varied by almost an order of magnitude between the studied species, ranging from 0.007 g h^{-1} for *O. europaea* to 0.083 g h^{-1} for *Liriodendron tulipifera*. At very low RWC values, below the desiccation point, the decrease is typically more pronounced and can reach near-zero values of g_{min}, when leaves dried below RWC 10% (Fig. 3).

Estimation of residual conductance along a dehydration time sequence

PV curve parameters (Table 1) were used to convert RWC thresholds into water potential (Ψ) values, obtaining the dynamics of a declining Ψ over time (Fig. S2). Converted Ψ values were used to estimate g_{min} at different dehydration levels, namely g_{min}_TLP, g_{min}_RWC$_{80\text{–}50}$, g_{min}_P$_{12}$, g_{min}_P$_{50}$, and g_{min}_P$_{88}$ (Table 2). Across the studied species, the absolute values of the different thresholded g_{min} estimations varied by more than an order of magnitude (Table 2; Fig. S3). However, for every species the magnitude of g_{min} based on these different thresholds followed the same order. The highest conductance was observed

New Phytologist

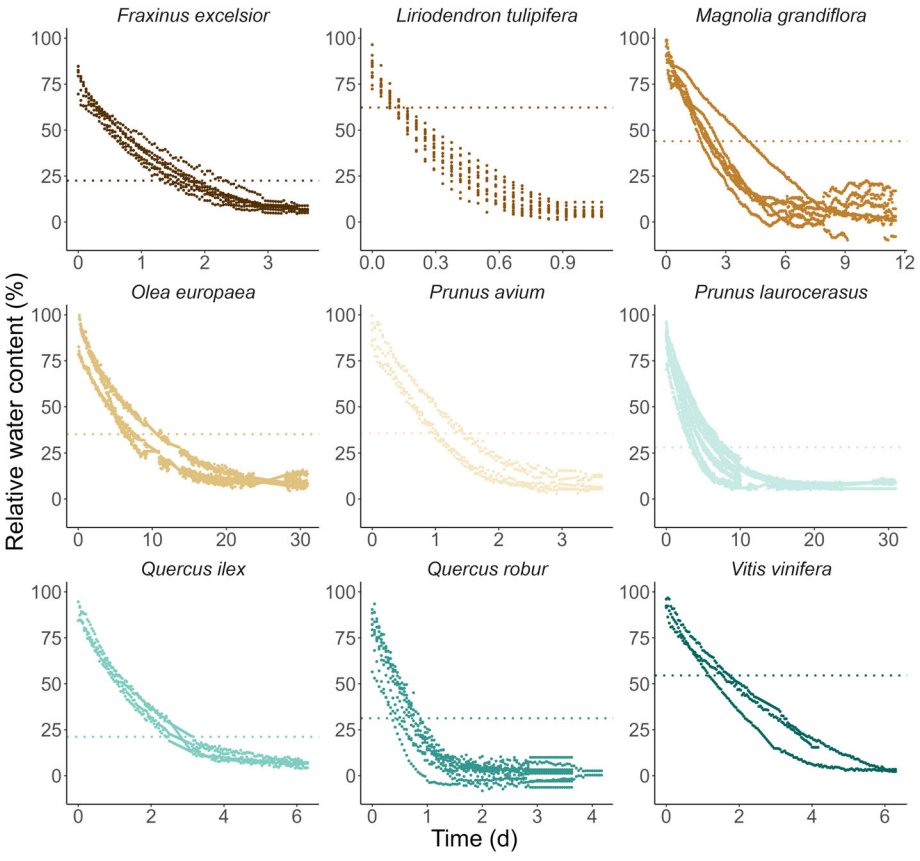

Fig. 1 Change in leaf relative water content (RWC) over elapsed time for each individual sample used in this study. Dashed horizontal lines represent the RWC at which the species reach P_{88}, the water content equivalent to the water potential inducing an 88% loss in hydraulic conductance. The apparent low initial RWC values for some samples result from a 120-min running mean filter to smooth the raw data.

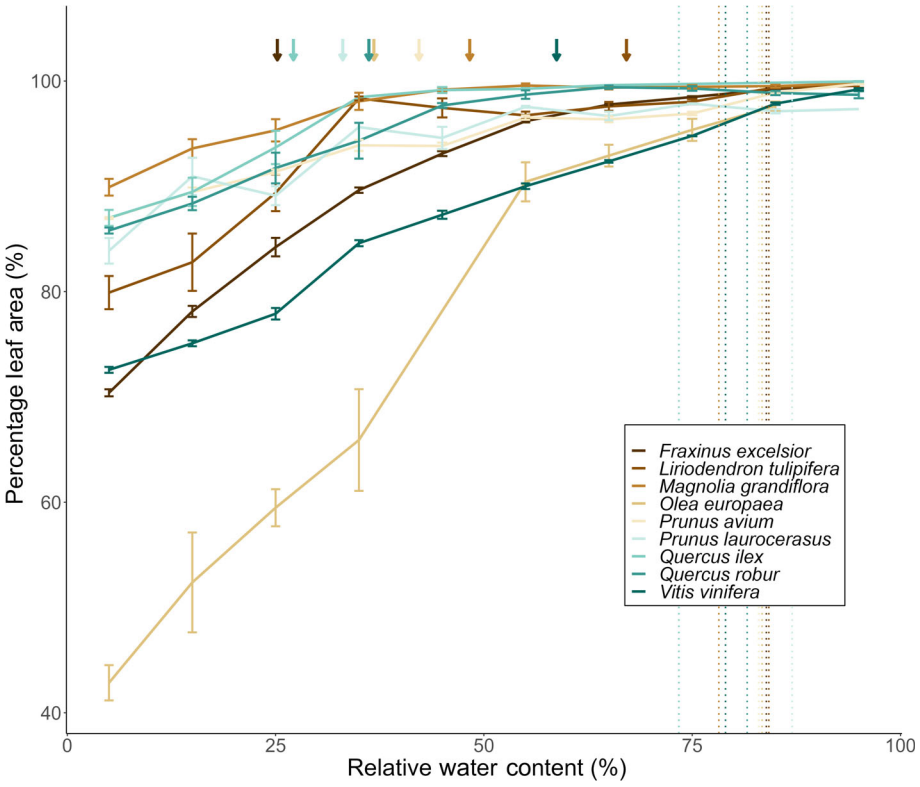

Fig. 2 Percentage of leaf area as a function of relative water content for the nine studied species. The projected leaf area, relative to the leaf area of a fully hydrated turgid leaf, declines with relative water content (RWC). Error bars indicate species mean values and SE for leaf area along segments of 10% RWC. Vertical dotted lines indicate turgor loss point (RWC_{TLP}), and arrows indicate RWC at P_{50} (RWC_P_{50}) for each species.

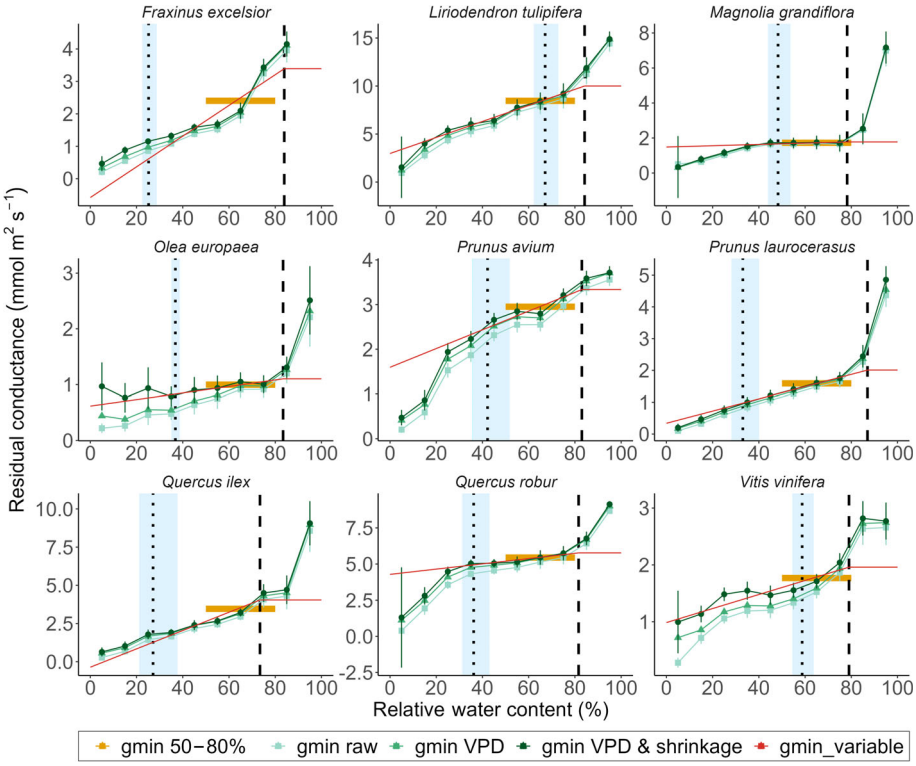

Fig. 3 Changes in residual conductance under declining relative water content. Species means of g_{min} values computed for each range of relative water content (RWC) with no correction (green square), with correction for vapor pressure deficit (VPD) only (green triangle), with correction for VPD & shrinkage (green circle). A detailed description of both corrections is provided in the Materials and Methods section. Orange bars represent the mean value of g_{min} between 50% and 80% RWC. Red lines represent the fitted values of g_{min} used as input for the dynamic computation of 'g_{min}_variable' in the SurEau model. Vertical dashed lines indicate RWC_TLP, and vertical dotted lines indicate RWC_P50. Blue shaded boxes indicate the ranges between P_{12} and P_{88}. Error bars indicate SE. Note the *y*-axis is defined differently for each species.

before TLP when leaves were not stressed. Then, the residual conductance decreased in sequence, with the g_{min} values estimated at TLP always higher than those measured between 50% and 80% of RWC, which were always higher than the estimation at different hydraulic dysfunction thresholds (Fig. S3). We found a significant effect of g_{min} computation method when considering all species ($P = 5.852e\text{-}07$).

Leaf minimum conductance at TLP showed the highest estimations with a mean value across all species of 3.78 ± 0.90 mmol m^{-2} s^{-1} (mean ± SE). As expected, given the decline in g_{min} values over leaf dehydration, g_{min} values thresholded at water statuses inducing P_{12}, P_{50}, and P_{88} declined sequentially across species with average values of 2.79 ± 0.893, 2.57 ± 0.87, and 2.42 ± 0.84 mmol m^{-2} s^{-1}, respectively. Estimates of g_{min} using the range 80–50% RWC provided a mean value of 3.25 ± 0.78 mmol m^{-2} s^{-1}, which was closer to the g_{min} values estimated at P_{12}, and both estimations were closely correlated to each other ($r = 0.97$; $P \leq 0.001$). Indeed, despite showing differences in g_{min} absolute values, all g_{min} estimates using different physiological and RWC thresholds were significantly correlated with each other (Table S3). Across species, we observed a positive correlation ($r = 0.87$; $P \leq 0.005$) between the modulus of elasticity (ε) and RWC_TLP. Yet, PV-curve parameters were not correlated with different g_{min} estimates (Table S3).

Impact of g_{min} on the time to hydraulic failure

The measured THF, defined as time to reach RWC_P_{88}, of detached leaves varied from 0.12 ± 0.01 d in *L. tulipifera* to 8.52 ± 1.86 d in *O. europaea* (Fig. 4). The deciduous species systematically showed shorter THF than the evergreen species (Fig. 4). The results from SurEau models showed that taking into account different ways to estimate g_{min} values leads to variations in THF for a given species (Table 2). The largest differences between extreme values (i.e. between g_{min}_P88 and g_{min}_TLP) for a given species range from 0.06 d for *L. tulipifera* to 6.01 d for *Fraxinus excelsior* (Fig. 5).

We found a close relationship between the modelled vs measured THF (Fig. 6a). Estimations based on fixed g_{min} values tend to show a bigger scatter than estimations based on a variable g_{min}. Root mean square error (RMSE) analysis shows that using a variable g_{min} provides an overall better agreement between modelled and measured THF (Fig. 6b). The modelled THF using the range 80–50% RWC or the fixed g_{min}_P_{12} value also provided a relatively small RMSE (< 1) compared to THF estimations based on either g_{min}_TLP or g_{min}_P_{50}.

Discussion

Leaf minimum water conductance, previously interchangeably referred to as residual conductance, is a hydraulic trait that is becoming increasingly central to studies of drought resistance and drought-induced mortality. Until this study, the methodology for estimating this trait assumed that leaf minimum conductance remained constant for a given sample along dehydration. We estimated leaf water loss along a temporal sequence of drought stress, and demonstrated that residual conductance (g_{res}) varies during the dehydration process and therefore cannot be considered a constant trait. Given the continuous variation of g_{res} during dehydration, we propose to use physiologically informed

Table 2 Average values of leaf minimum conductance (g_{min}) and time to hydraulic failure (THF) for each species.

Species	g_{min}_$RWC_{80\text{-}50}$ (mmol m^{-2} s^{-1})	g_{min}_TLP (mmol m^{-2} s^{-1})	g_{min}_P_{12} (mmol m^{-2} s^{-1})	g_{min}_P_{50} (mmol m^{-2} s^{-1})	g_{min}_P_{88} (mmol m^{-2} s^{-1})	THF_ RWC_{80_50} (d)	THF_ TLP (d)	THF_ P_{12} (d)	THF_ P_{50} (d)	THF_ P_{88} (d)	THF_ variable (d)	THF_ observed (d)
Fraxinus excelsior	2.40 ± 0.52	3.39 ± 0.41	0.78 ± 0.17	0.61 ± 0.2	0.48 ± 0.23	1.43	1.02	4.39	5.56	07.03	3.48	1.74 ± 0.12
Liriodendron tulipifera	8.46 ± 0.42	10.00 ± 0.75	9.05 ± 0.67	8.58 ± 0.63	8.17 ± 0.6	0.29	0.25	0.27	0.29	0.30	0.27	0.12 ± 0.01
Magnolia grandiflora	1.93 ± 0.13	2.15 ± 0.05	1.77 ± 0.04	1.69 ± 0.05	1.62 ± 0.05	2.24	1.99	2.45	2.58	2.70	2.44	2.38 ± 0.75
Olea europaea	1.06 ± 0.01	1.22 ± 0.95	0.87 ± 0.28	0.85 ± 0.32	0.84 ± 0.36	6.08	5.29	7.40	7.53	7.64	6.62	8.53 ± 0.84
Prunus avium	2.95 ± 0.18	3.34 ± 0.19	2.68 ± 0.18	2.48 ± 0.19	2.34 ± 0.2	1.09	0.97	1.20	1.29	1.37	1.20	1.18 ± 0.12
Prunus laurocerasus	1.59 ± 0.12	2.01 ± 0.12	1.11 ± 0.14	0.97 ± 0.16	0.88 ± 0.17	4.57	3.62	6.54	7.43	8.22	6.43	5.62 ± 0.48
Quercus ilex	3.46 ± 0.54	4.04 ± 0.55	1.90 ± 0.29	1.27 ± 0.25	0.91 ± 0.24	1.74	1.50	3.12	4.66	6.45	3.66	2.75 ± 0.14
Quercus robur	5.59 ± 0.14	5.93 ± 0.69	5.13 ± 0.21	4.98 ± 0.19	4.88 ± 0.22	0.57	0.54	0.62	0.64	0.65	0.61	0.58 ± 0.08
Vitis vinifera	1.77 ± 0.14	1.96 ± 0.24	1.77 ± 0.22	1.71 ± 0.21	1.66 ± 0.2	1.28	1.16	1.28	1.33	1.37	1.33	1.49 ± 0.16

'g_{min}_' denotes minimum conductance at different thresholds. 'THF_' denotes time to hydraulic failure at different thresholds. 80–50% RWC, 80% to 50% relative water content; TLP, turgor loss point; P_{12}, 12% loss of hydraulic conductivity; P_{50}, 50% loss of hydraulic conductivity; P_{88}, 88% loss of hydraulic conductivity. Reported error values are SE.

or water content-based thresholds for its estimation. Therefore, our study urges distinguishing the terms 'residual' conductance, as a dynamic water loss after stomatal closure, and 'minimum' conductance, which imply the use of established boundaries for its estimation. In this context, we estimated g_{min} at physiologically relevant thresholds distributed along a temporal sequence of drought stress and demonstrated that g_{min} estimations vary during leaf dehydration. We subsequently show that, depending on the threshold at which g_{min} is estimated, the drought survival time estimated by our model varies considerably. These results have important implications for better estimating the risk of hydraulic failure during drought and predicting the impact of climate change on species survival and distribution.

Residual conductance varies during dehydration

Residual conductance decreases continuously during the entire dehydration process. Such declines in conductance rates were observed in all the studied species. Decreases in leaf water conductance were still observed after normalizations by projected leaf area corrected for leaf shrinkage, which is a main variable for the calculation of g_{min} (see Eqn 2). An effect of shrinkage on the reduction of g_{min} could be expected since it has been shown that leaf thickness during dehydration is negatively correlated with hydraulic conductance (K_{leaf}) on 14 diverse species (Scoffoni *et al.*, 2014). However, leaf surface shrinkage seems to be less effective in driving decreases in residual conductance estimations, especially at the first stages of dehydration since leaf shrinkage was relatively limited in the range of RWC between 100% and 50%. Similarly, the investigation of the effect of VPD shifts during conductance measurements, which is considered here to be affected mainly by the drop in water potential inside the leaf, showed that even though the decrease is less pronounced after correction, it does not change the direction of the slope. Overall, corrections of leaf shrinkage and dehydration-induced leaf-to-air VPD slightly increased our residual conductance estimations. Yet, the dynamics of residual conductance decrease under declining RWC or dehydration time remained unaffected after correcting for both potential drivers. Taking into consideration the main finding that residual conductance is not steady during dehydration, we provide solutions for calculating g_{min} either at fixed values (based on RWC or physiological thresholds) or dynamically during a dehydration process. Altogether, these results demonstrate that g_{min} is not a constant hydraulic trait for a given species and varies in time during a drought event. We therefore suggest the use of physiology-based boundaries for its calculation.

The variation of leaf water conductance during dehydration observed in this study is in line with several studies that evidenced contrasted responses of leaf weight loss rates for different water stress conditions. For instance, it has been shown that drought significantly impacts the water loss rate for both young and mature tea (*Camellia sinensis*) leaves (Chen *et al.*, 2020). The process leading to this variation during a stress gradient is not fully known and needs to be further investigated. We can hypothesize that it could come from incompletely closed stomata (Machado *et al.*, 2021), driving stomatal patchiness, which is the irregular closing of

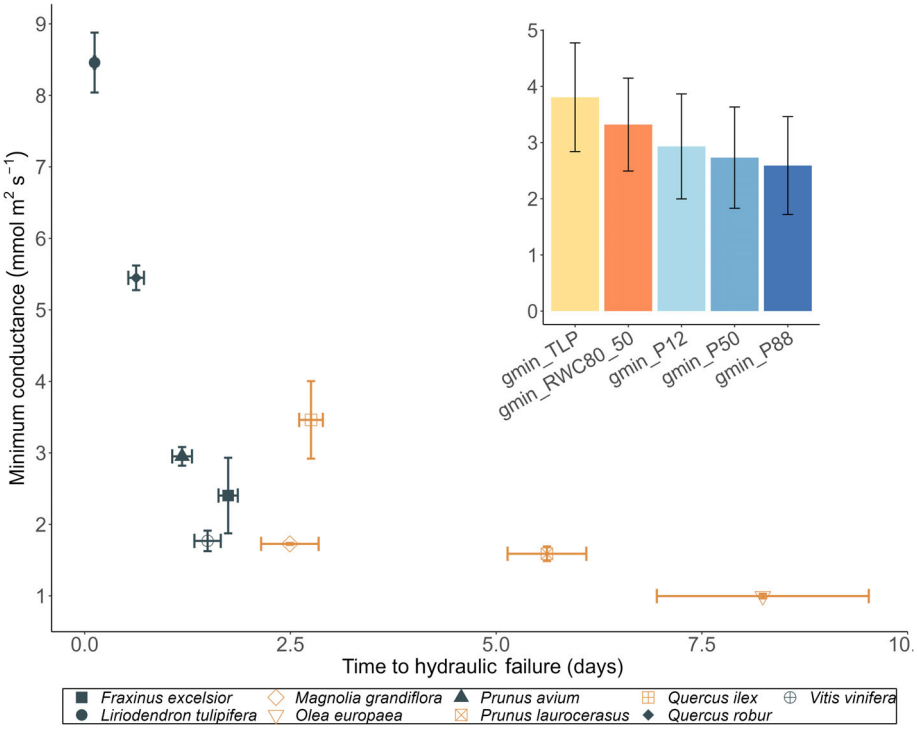

Fig. 4 Relationship between measured time to hydraulic failure (THF) and leaf minimum conductance (g_{min}) corrected for shrinkage and vapor pressure deficit variation. For each sample, g_{min} is computed for a relative water content between 50% and 80%. Error bars represent SE. Deciduous species are represented by blue symbols and evergreen species by yellow symbols. Inset represents averaged g_{min} values computed at different thresholds.

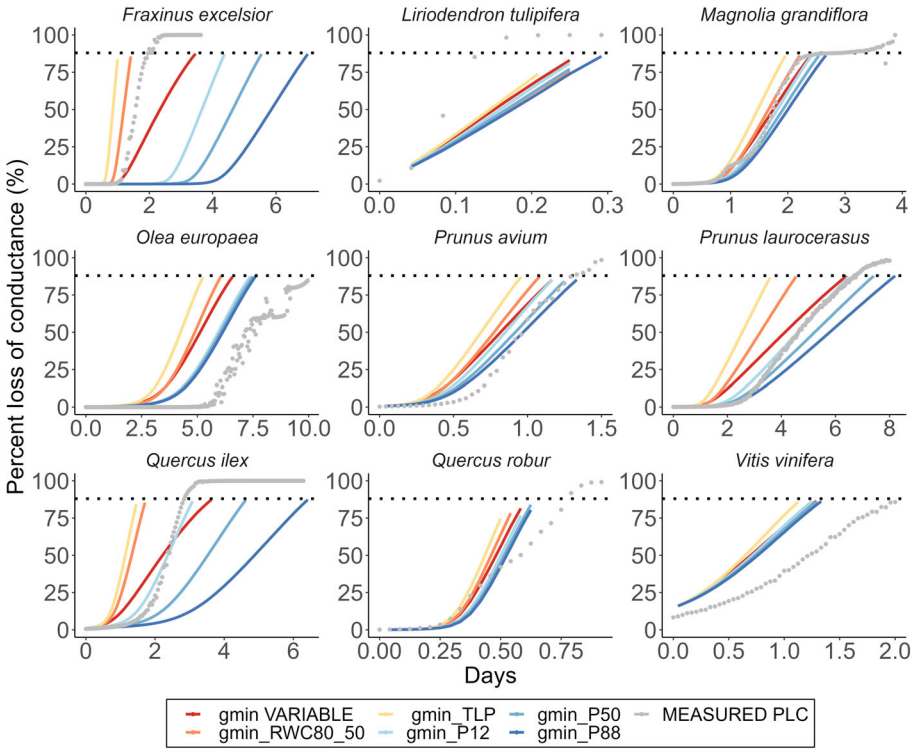

Fig. 5 Changes in modelled and measured percent loss of conductance (PLC) in relation to time. Colored lines represent model results for different types of computation of g_{min}. Gray points represent the measured value of PLC (estimated from relative water content (RWC), with the pressure–volume curve). Dashed black lines represent the value of P_{88} (defined as the threshold for the time to hydraulic failure). Note the *x*-axis is defined differently for each species.

stomata over the entire surface of the leaf (Mott & Buckley, 1998). Along with such mechanisms deriving from stomatal activity, features of the cuticular structure could also explain such variation in residual conductance. More specifically, the main effect of the cuticle on g_{min} could come from a modification of the structure by the elongation of the molecules composing the cuticle (Shepherd & Wynne Griffiths, 2006; Lewandowska *et al.*, 2020) or *de novo* cuticular wax biosynthesis (Premachandra *et al.*, 1991). In this respect, a study on *Nicotiana glauca* leaves described a strong effect of water stress on leaf permeance by the accumulation of waxes during stress

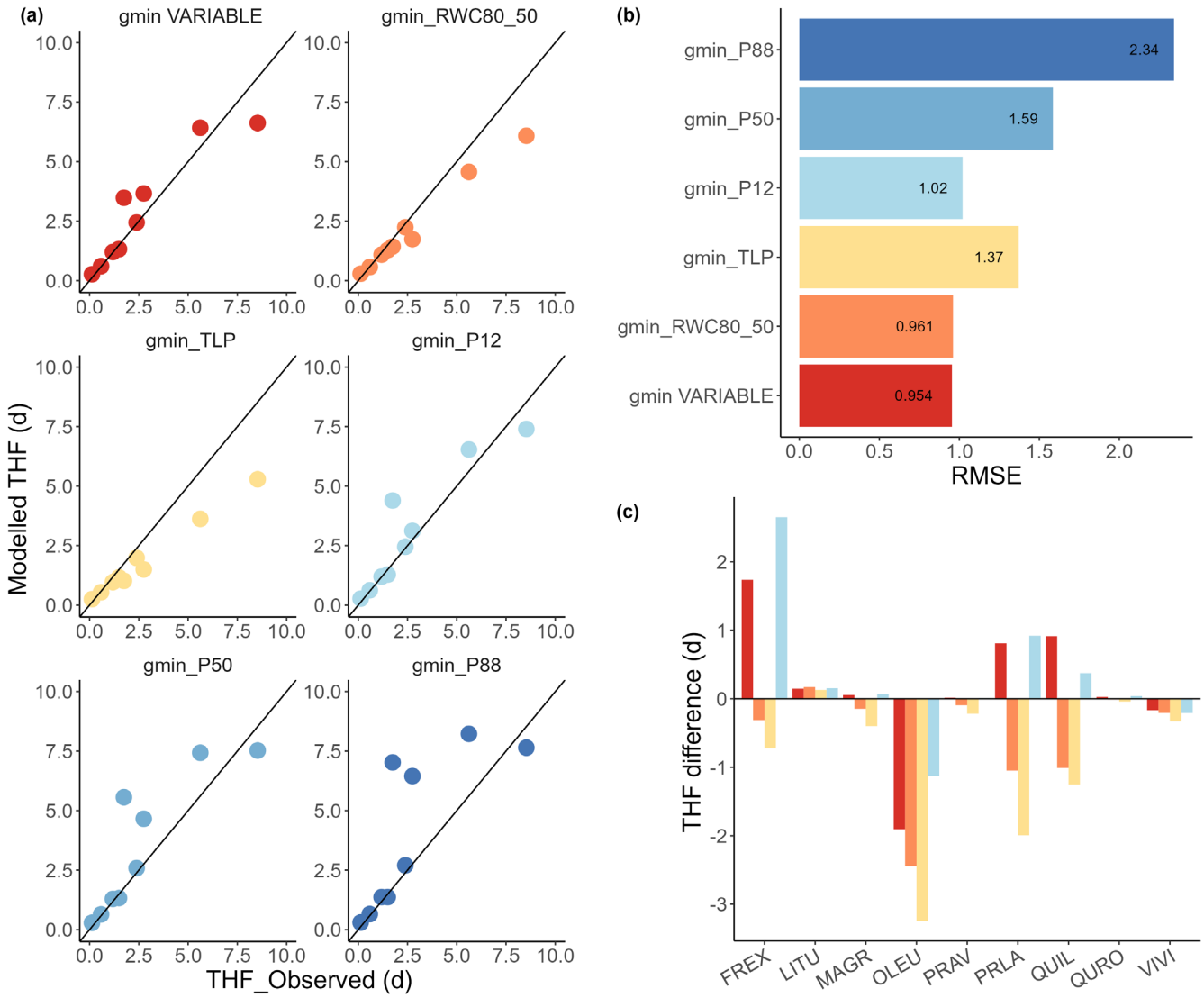

Fig. 6 Relationship between modelled and observed time to hydraulic failure using different computations of g_{min}. (a) Comparison between modeled and measured time to hydraulic failure (THF) across different g_{min} estimations. THF is defined as the time to reach P_{88}. Each point corresponds to the average of THF for each of the studied species. Black lines indicate a 1 : 1 relationship. (b) Root mean square error (RMSE) comparing the performance of the models using different g_{min} values. (c) Difference between modelled and observed THF for each species, and color codes, corresponding to different g_{min} values, are the same as in panel b. Species abbreviation codes are included in Table 1.

(Cameron *et al.*, 2006). Moreover, a recent study on *Nicotiana benthamiana* has shown effective responses to drought stress by changes in the composition and accumulation of cuticular waxes, resulting in increases in cuticular thickness (Asadyar *et al.*, 2024). However, such accumulation of waxes during stress might mostly drive seasonal changes in residual conductance and would not explain the variation observed in our study, which occurred over a much shorter time frame.

Despite the relevance of the cuticular features previously presented, several studies show a weak effect of the amount of cuticle on minimal conductance, which would suggest that the amount of cuticular waxes is not the only driver of the decline in g_{min} observed here. For example, no difference in the amount of wax has been found for *Quercus coccifera* growing in different environments (Bueno *et al.*, 2019). Additionally, a recent study found no difference in permeance for a *Populus* × *canescens* clone while the authors measured 10-fold differences in wax composition (Grünhofer *et al.*, 2022). These findings would suggest that the variation in residual conductance is substantially driven by the dynamics of stomatal closure during dehydration. Further work is, however, needed to investigate the extent of the role played by a modification of the structure or composition of the cuticle in this variation.

Impact of the variation in minimum conductance estimates on time-to-death prediction

Decreases in leaf g_{min} values are observed even at mild stress levels when leaves are still hydraulically connected to the stem (typically

between TLP and P_{50}). This variation has a direct consequence on the speed of diminution of plant water content, and therefore, a direct influence on the quality of the prediction of the THF, which is a prominent proxy of plant survival under drought, using mechanistic models based on hydraulic traits (Cochard *et al.*, 2021; Ruffault *et al.*, 2022a). The effect of a variable g_{min} on the THF estimations is, however, more or less pronounced for the different species. For instance, the modelled THF for species having the lowest resistance to embolism (i.e. the highest RWC_P_{88}), like *L. tulipifera* or *Vitis vinifera*, was less impacted by the variation in g_{min} values. Conversely, the species that show higher resistance to embolism, like *F. excelsior* or *Quercus ilex*, present large g_{min}-induced variations in modelled THF, suggesting that the variation in residual conductance could be more relevant in predicting hydraulic failure in species with a more resistant hydraulic apparatus and hence a larger safety margin (Fig. S4). Given the importance of g_{min} on the pace to cross the safety margin (Petek-Petrik *et al.*, 2023), a variable residual conductance could be more relevant in species with wider margins, where the speed of water loss would be more relevant to reaching hydraulic failure.

Even though the simulations in this study are based on several simplifying assumptions and on a limited set of traits, the absolute values of the modelled THF showed overall good agreement with the observed THF, which is the time to reach water contents inducing P_{88} directly measured during the dehydration experiment. One of the main simplifying assumptions we made in the model parametrization is that the vulnerability to cavitation is similar between leaf and stem. However, we know that many plants differ from this assumption and exhibit hydraulic vulnerability segmentation between their organs. For instance, several studies reported significant segmentation for species closely related to our selection of species. Leaves are slightly more vulnerable to cavitation (typically below 1 MPa) for most species; for example, segmentation of −0.67 MPa is reported for *Quercus douglasii* (Skelton *et al.*, 2019), *c.* −0.8 MPa for *V. vinifera* (Hochberg *et al.*, 2016), *c.* −0.8 MPa for *Juglans regia* (Tyree *et al.*, 1993), −0.9 MPa for *Fraxinus mandshurica* (Song *et al.*, 2022), and between −0.73 MPa (Li *et al.*, 2020) and −0.91 MPa (Rodriguez-Dominguez *et al.*, 2018) for *O. europaea*.

Despite the previously observed trend, where leaves are more sensitive to drought than stems, some species included in our study have shown the opposite pattern, with more drought-resistant leaves. For instance, in *L. tulipifera*, two different studies have reported that leaves are more resistant than stems with leaf-to-stem segmentations of +0.47 MPa (Li *et al.*, 2020) and +0.68 MPa (Guan *et al.*, 2022). Additionally, *Prunus avium* and *Quercus robur* also have positive leaf-to-stem hydraulic vulnerability segmentations of +1.84 MPa and +0.31 MPa, respectively (Guan *et al.*, 2022). Such a positive leaf-to-stem hydraulic vulnerability segmentation might explain why our model output overestimated the THF for these species (Fig. 5). Even at the level of the single organ, the estimation of THF is the result of several parameters, among which residual conductance and its temporal variation can play a major role. Leaves might however be disconnected before significant stem cavitation (RWC_P_{50}). This implies that only the variation of g_{min} above this point of disconnection is relevant to estimate time-to-death at the plant level. Given that some species studied here showed a positive leaf-to-stem vulnerability segmentation, the use of stem P_{50} as a reference threshold for minimum conductance could be interesting, despite belonging to a different organ, since it informs residual water losses that occur at earlier stages of drought-induced hydraulic dysfunction.

Toward a standardized methodology to estimate g_{min}

The data acquisition system and the linked computation pipeline described in this study provided an accurate, versatile, cheap, and time-efficient methodology to compute g_{min}, even for a large number of samples. Using a standardized averaging procedure, like the one implemented in this pipeline, combined with data oversampling permits a good fit of the raw data even if the signal is noisy (e.g. due to movement of the sample caused by ventilation). We show that accounting for tissue shrinkage and the water-potential-induced changes in VPD during drought has only a minor effect on the calculation of residual conductance, particularly within the RWC range where leaves remain hydraulically connected to the stem.

Our approach, which dynamically investigates the contributions of all the aspects involved in g_{min} computation, describes more accurately the phenomenon occurring *in vivo* during dehydration and demonstrates its impact on the output of models considering hydraulic traits. However, this approach is not solely based on the measurement of mass loss during dehydration. A prior knowledge of several other traits, such as PV curves and vulnerability curve parameters, is required. It remains important, however, to have a reproducible method to compute a g_{min} value representative of a sample along a dehydration threshold even when physiological data are not available. In such cases, RWC can be used as a convenient metric to specify relevant thresholds for conductance estimations. If physiological or RWC thresholds are specified, then g_{min} values could be considered as a measurable and more stable trait. For instance, the use of a range between stomatal closure and leaf disconnection provides an estimation that integrates over the whole dehydration range. These thresholds are typically close to RWC of 80% and 50%, respectively, and we show that such a range produces a good estimation of THF as compared to the observed values during the experiment. We therefore encourage using the minimum conductance estimated between those values (g_{min}_RWC_{80_50}) as a relevant trait when comparing species or genotypes over the entire course of dehydration, and without preliminary knowledge of other physiological traits. Other thresholds might be relevant for different types of studies. We would recommend that, for future reports of g_{min}, researchers make available both the threshold (or range of RWC) used for the computation and the raw data used to compute g_{min} so that future studies could harmonize computations if needed. The methodology presented in this study is a step toward a unified framework for studying residual water losses and minimum conductance values for many organs, such as leaves, branches, roots, and flowers.

Acknowledgements

The authors wish to thank Anne-Isabelle Gravel and Gaëlle Capdeville for their help in the glasshouse and in the laboratory and Annabel Porte for thoughtful advice. All measurements were performed at the PHENOBOIS platform. This study received financial support from the French government in the framework of the IdEX Bordeaux University 'Investments for the Future' program/GPR Bordeaux Plant Sciences. Financial support was also received from the French National Research Agency (ANR) in the frame of the Investments for the future Program, within the Cluster of Excellence COTE(ANR-10-LABX-0045), project LEAFSHED.

Competing interests

None declared.

Author contributions

RB, ST, SD, HC, JMT-R and NKM-SP contributed to the design of the study and the interpretation of the results; RB and ST performed data collection and analysis; HC carried out the simulations.; CP performed pressure–volume curves and provided help in the glasshouse; GF and XPB wrote the software for the computation of g_{min}; RB wrote the data acquisition software; RB, ST and SD wrote the manuscript with help from all authors.

ORCID

Xavier Paul Bouteiller https://orcid.org/0000-0001-8621-383X
Régis Burlett https://orcid.org/0000-0001-8289-5757
Hervé Cochard https://orcid.org/0000-0002-2727-7072
Sylvain Delzon https://orcid.org/0000-0003-3442-1711
Guillaume Forget https://orcid.org/0009-0000-4778-3194
Nicolas K. Martin-StPaul https://orcid.org/0000-0001-7574-0108
Camille Parise https://orcid.org/0000-0001-5222-4928
José M. Torres-Ruiz https://orcid.org/0000-0003-1367-7056
Santiago Trueba https://orcid.org/0000-0001-8218-957X

Data availability

Codes developed for data acquisition (software 'cuticular' for Windows) and computation of raw residual conductance (project 'gminComputation' is developed as a console version in python, and 'g_Residual' is a script written in R language) are available in the following public Gitlab repository: https://gitub.u-bordeaux.fr/phenobois. Data specifically used for this manuscript are available on the dataverse https://recherche.data.gouv.fr; doi: 10.57745/S11KRP.

References

Allen CD, Breshears DD. 1998. Drought-induced shift of a forest–woodland ecotone: Rapid landscape response to climate variation. *Proceedings of the National Academy of Sciences, USA* **95**: 14839–14842.

Arend M, Link RM, Patthey R, Hoch G, Schuldt B, Kahmen A. 2021. Rapid hydraulic collapse as cause of drought-induced mortality in conifers. *Proceedings of the National Academy of Sciences, USA* **118**: e2025251118.

Asadyar L, de Felippes FF, Bally J, Blackman CJ, An J, Sussmilch FC, Moghaddam L, Williams B, Blanksby SJ, Brodribb TJ *et al.* 2024. Evidence for within-species transition between drought response strategies in *Nicotiana benthamiana*. *New Phytologist* **244**: 464–476.

Barnard DM, Bauerle WL. 2013. The implications of minimum stomatal conductance on modeling water flux in forest canopies. *Journal of Geophysical Research: Biogeosciences* **118**: 1322–1333.

Billon LM, Blackman CJ, Cochard H, Badel E, Hitmi A, Cartailler J, Souchal R, Torres-Ruiz JM. 2020. The DroughtBox: a new tool for phenotyping residual branch conductance and its temperature dependence during drought. *Plant, Cell & Environment* **43**: 1584–1594.

Boyer JS, Wong SC, Farquhar GD. 1997. CO_2 and water vapor exchange across leaf cuticle (epidermis) at various water potentials. *Plant Physiology* **114**: 185–191.

Brodribb TJ, Cochard H, Dominguez CR. 2019. Measuring the pulse of trees; using the vascular system to predict tree mortality in the 21st century. *Conservation Physiology* **7**: 1–7.

Brodribb TJ, Holbrook NM. 2003. Changes in leaf hydraulic conductance during leaf shedding in seasonally dry tropical forest. *New Phytologist* **158**: 295–303.

Bueno A, Sancho-Knapik D, Gil-Pelegrín E, Leide J, Peguero-Pina JJ, Burghardt M, Riederer M. 2019. Cuticular wax coverage and its transpiration barrier properties in *Quercus coccifera* L. leaves: does the environment matter? *Tree Physiology* **40**: 827–840.

Burlett R, Parise C, Capdeville G, Cochard H, Lamarque LJ, King A, Delzon S. 2022. Measuring xylem hydraulic vulnerability for long-vessel species: an improved methodology with the flow centrifugation technique. *Annals of Forest Science* **79**: 5.

Cameron KD, Teece MA, Smart LB. 2006. Increased accumulation of cuticular wax and expression of lipid transfer protein in response to periodic drying events in leaves of tree tobacco. *Plant Physiology* **140**: 176–183.

Carnicer J, Coll M, Ninyerola M, Pons X, Sánchez G, Peñuelas J. 2011. Widespread crown condition decline, food web disruption, and amplified tree mortality with increased climate change-type drought. *Proceedings of the National Academy of Sciences, USA* **108**: 1474–1478.

Chen M, Zhu X, Zhang Y, Du Z, Chen X, Kong X, Sun W, Chen C. 2020. Drought stress modify cuticle of tender tea leaf and mature leaf for transpiration barrier enhancement through common and distinct modes. *Scientific Reports* **10**: 1–12.

Choat B, Jansen S, Brodribb TJ, Cochard H, Delzon S, Bhaskar R, Bucci SJ, Feild TS, Gleason SM, Hacke UG. 2012. Global convergence in the vulnerability of forests to drought. *Nature* **491**: 752–755.

Cochard H. 2002. A technique for measuring xylem hydraulic conductance under high negative pressures. *Plant, Cell & Environment* **25**: 815–819.

Cochard H, Pimont F, Ruffault J, Martin-StPaul N. 2021. SurEau: a mechanistic model of plant water relations under extreme drought. *Annals of Forest Science* **78**: 55.

Creek D, Lamarque LJ, Torres-Ruiz JM, Parise C, Burlett R, Tissue DT, Delzon S. 2020. Xylem embolism in leaves does not occur with open stomata: evidence from direct observations using the optical visualization technique. *Journal of Experimental Botany* **71**: 1151–1159.

Delf EM. 1912. Transpiration in succulent plants. *Annals of Botany* **26**: 409–442.

Delzon S, Cochard H. 2014. Recent advances in tree hydraulics highlight the ecological significance of the hydraulic safety margin. *New Phytologist* **203**: 355–358.

Duursma RA, Blackman CJ, Lopéz R, Martin-StPaul NK, Cochard H, Medlyn BE. 2018. On the minimum leaf conductance: its role in models of plant water use, and ecological and environmental controls. *New Phytologist* **221**: 693–705.

Grünhofer P, Herzig L, Sent S, Zeisler-Diehl VV, Schreiber L. 2022. Increased cuticular wax deposition does not change residual foliar transpiration. *Plant, Cell & Environment* **45**: 1157–1171.

Guan X, Werner J, Cao K-F, Pereira L, Kaack L, McAdam SAM, Jansen S. 2022. Stem and leaf xylem of angiosperm trees experiences minimal embolism in temperate forests during two consecutive summers with moderate drought. *Plant Biology* **24**: 1208–1223.

Hammond WM, Williams AP, Abatzoglou JT, Adams HD, Klein T, López R, Sáenz-Romero C, Hartmann H, Breshears DD, Allen CD. 2022. Global field

observations of tree die-off reveal hotter-drought fingerprint for Earth's forests. *Nature Communications* **13**: 1761.

Hochberg U, Albuquerque C, Rachmilevitch S, Cochard H, David-Schwartz R, Brodersen CR, McElrone A, Windt CW. 2016. Grapevine petioles are more sensitive to drought induced embolism than stems: evidence from *in vivo* MRI and microcomputed tomography observations of hydraulic vulnerability segmentation. *Plant, Cell & Environment* **39**: 1886–1894.

Kala J, De Kauwe MG, Pitman AJ, Medlyn BE, Wang Y-P, Lorenz R, Perkins-Kirkpatrick SE. 2016. Impact of the representation of stomatal conductance on model projections of heatwave intensity. *Scientific Reports* **6**: 23418.

Kerstiens G. 1996. Signalling across the divide: a wider perspective of cuticular structure-function relationships. *Trends in Plant Science* **1**: 125–129.

Koide RT, Robichaux RH, Morse SR, Smith CM. 2000. Plant water status, hydraulic resistance and capacitance. In: Pearcy RW, Ehleringer JR, Mooney HA, Rundel PW, eds. *Plant physiological ecology: field methods and instrumentation*. Dordrecht, the Netherlands: Springer Netherlands, 161–183.

Lamarque LJ, Corso D, Torres-Ruiz JM, Badel E, Brodribb TJ, Burlett R, Charrier G, Choat B, Cochard H, Gambetta GA *et al.* 2018. An inconvenient truth about xylem resistance to embolism in the model species for refilling *Laurus nobilis* L. *Annals of Forest Science* **75**: 88.

Lewandowska M, Keyl A, Feussner I. 2020. Wax biosynthesis in response to danger: its regulation upon abiotic and biotic stress. *New Phytologist* **227**: 698–713.

Li S, Feifel M, Karimi Z, Schuldt B, Choat B, Jansen S. 2016. Leaf gas exchange performance and the lethal water potential of five European species during drought. *Tree Physiology* **36**: 179–192.

Li X, Delzon S, Torres-Ruiz J, Badel E, Burlett R, Cochard H, Jansen S, King A, Lamarque LJ, Lenoir N *et al.* 2020. Lack of vulnerability segmentation in four angiosperm tree species: evidence from direct X-ray microtomography observation. *Annals of Forest Science* **77**: 1–12.

Machado R, Loram-Lourenço L, Farnese FS, Alves RDFB, de Sousa LF, Silva FG, Filho SCV, Torres-Ruiz JM, Cochard H, Menezes-Silva PE. 2021. Where do leaf water leaks come from? Trade-offs underlying the variability in minimum conductance across tropical savanna species with contrasting growth strategies. *New Phytologist* **229**: 1415–1430.

Mantova M, Cochard H, Burlett R, Delzon S, King A, Rodriguez-Dominguez CM, Ahmed MA, Trueba S, Torres-Ruiz JM. 2023. On the path from xylem hydraulic failure to downstream cell death. *New Phytologist* **237**: 793–806.

Márquez DA, Stuart-Williams H, Farquhar GD, Busch FA. 2022. Cuticular conductance of adaxial and abaxial leaf surfaces and its relation to minimum leaf surface conductance. *New Phytologist* **233**: 156–168.

Martin-StPaul N, Delzon S, Cochard H. 2017. Plant resistance to drought depends on timely stomatal closure. *Ecology Letters* **20**: 1437–1447.

Mott KA, Buckley TN. 1998. Stomatal heterogeneity. *Journal of Experimental Botany* **49**: 407–417.

Nobel PS. 2009. Chapter 2 – water. In: Nobel PS, ed. *Physicochemical and environmental plant physiology*. San Diego, CA, USA: Academic Press, 44–99.

Pearcy RW, Schulze E-D, Zimmermann R. 1989. Measurement of transpiration and leaf conductance. In: Pearcy RW, Ehleringer JR, Mooney HA, Rundel PW, eds. *Plant physiological ecology: field methods and instrumentation*. Dordrecht, the Netherlands: Springer Netherlands, 137–160.

Petek-Petrik A, Petrík P, Lamarque LJ, Cochard H, Burlett R, Delzon S. 2023. Drought survival in conifer species is related to the time required to cross the stomatal safety margin. *Journal of Experimental Botany* **74**: 6847–6859.

Premachandra GS, Saneoka H, Kanaya M, Ogata S. 1991. Cell membrane stability and leaf surface wax content as affected by increasing water deficits in maize. *Journal of Experimental Botany* **42**: 167–171.

R Core Team. 2022. *R: a language and environment for statistical computing*. Vienna, Austria: R Foundation for Statistical Computing.

Rodriguez-Dominguez CM, Carins Murphy MR, Lucani C, Brodribb TJ. 2018. Mapping xylem failure in disparate organs of whole plants reveals extreme resistance in olive roots. *New Phytologist* **218**: 1025–1035.

Ruffault J, Pimont F, Cochard H, Dupuy J-L, Martin-StPaul N. 2022a. SurEau-Ecos v.2.0: a trait-based plant hydraulics model for simulations of plant water status and drought-induced mortality at the ecosystem level. *Geoscientific Model Development* **15**: 5593–5626.

Ruffault J, Pimont F, Dupuy JL. 2022b. SurEau-Ecos-FMC: mechanistic modelling of fuel moisture content (FMC) at leaf and canopy scale under extreme drought. *Journal of Advances in Forest Fire Research* **4**: 1318–1322.

Sack L, Pasquet-Kok J, Bartlett M. 2010. *Leaf pressure–volume curve parameters protocol*. PROMETHEUS Wiki.

Sack L, Scoffoni C. 2010. Minimum epidermal conductance (gmin, a.k.a. cuticular conductance). PROMETHEUS Wiki.

Schönherr J, Mérida T. 1981. Water permeability of plant cuticular membranes: the effects of humidity and temperature on the permeability of non-isolated cuticles of onion bulb scales. *Plant, Cell & Environment* **4**: 349–354.

Scoffoni C, Vuong C, Diep S, Cochard H, Sack L. 2014. Leaf shrinkage with dehydration: coordination with hydraulic vulnerability and drought tolerance. *Plant Physiology* **164**: 1772–1788.

Shepherd T, Wynne Griffiths D. 2006. The effects of stress on plant cuticular waxes. *New Phytologist* **171**: 469–499.

Skelton RP, Anderegg LDL, Papper P, Reich E, Dawson TE, Kling M, Thompson SE, Diaz J, Ackerly DD. 2019. No local adaptation in leaf or stem xylem vulnerability to embolism, but consistent vulnerability segmentation in a North American oak. *New Phytologist* **223**: 1296–1306.

Song J, Trueba S, Yin X-H, Cao K-F, Brodribb TJ, Hao G-Y. 2022. Hydraulic vulnerability segmentation in compound-leaved trees: evidence from an embolism visualization technique. *Plant Physiology* **189**: 204–214.

Sperry JS, Donnelly JR, Tyree MT. 1988. A method for measuring hydraulic conductivity and embolism in xylem. *Plant, Cell & Environment* **11**: 35–40.

Stålfelt MG. 1956. Die cuticuläre transpiration. In: Adriani MJ, ed. *Pflanze und Wasser/water relations of plants. Handbuch der Pflanzenphysiologie/encyclopedia of plant physiology*. Berlin, Heidelberg, Germany: Springer.

Torres-Ruiz JM, Cochard H, Delzon S, Boivin T, Burlett R, Cailleret M, Corso D, Delmas CEL, Caceres M, Diaz-Espejo A *et al.* 2024. Plant hydraulics at the heart of plant, crops and ecosystem functions in the face of climate change. *New Phytologist* **241**: 984–999.

Trueba S, Pan R, Scoffoni C, John GP, Davis SD, Sack L. 2019. Thresholds for leaf damage due to dehydration: declines of hydraulic function, stomatal conductance and cellular integrity precede those for photochemistry. *New Phytologist* **223**: 134–149.

Tyree MT, Cochard H, Cruiziat P, Sinclair B, Ameglio T. 1993. Drought-induced leaf shedding in walnut: evidence for vulnerability segmentation. *Plant, Cell & Environment* **16**: 879–882.

Tyree MT, Hammel HT. 1972. The measurement of the turgor pressure and the water relations of plants by the pressure-bomb technique. *Journal of Experimental Botany* **23**: 267–282.

Urli M, Porté AJ, Cochard H, Guengant Y, Burlett R, Delzon S. 2013. Xylem embolism threshold for catastrophic hydraulic failure in angiosperm trees. *Tree Physiology* **33**: 672–683.

Vesala T, Sevanto S, Grönholm T, Salmon Y, Nikinmaa E, Hari P, Hölttä T. 2017. Effect of leaf water potential on internal humidity and CO_2 dissolution: reverse transpiration and improved water use efficiency under negative pressure. *Frontiers in Plant Science* **8**: 54.

Supporting Information

Additional Supporting Information may be found online in the Supporting Information section at the end of the article.

Fig. S1 Changes in individual leaf mass raw values over elapsed time.

Fig. S2 Changes in mean modelled water potential values over elapsed time.

Fig. S3 Minimum conductance (g_{min}) estimations based on physiological and water content thresholds for each species.

Fig. S4 Relationship between hydraulic safety margin and the difference in time to hydraulic failure between stomatal closure and plant death.

Methods S1 Detailed description of the minimum conductance measurement setup.

Table S1 Additional physiological variables used for the parameterization of the SurEau model.

Table S2 Analysis of variance of percent leaf area as a function of 10% relative water content intervals and species.

Table S3 Coordination between pressure–volume curve parameters and different minimum conductance estimations.

Please note: Wiley is not responsible for the content or functionality of any Supporting Information supplied by the authors. Any queries (other than missing material) should be directed to the *New Phytologist* Central Office.